ISSN 0208-7774 TRIBOLOGIA 4/2020 p. 7–16
DOI: 10.5604/01.3001.0014.5891

Artur OLSZEWSKI[*], Grzegorz ŻYWICA[**], Tomasz ŻOCHOWSKI[***]

DESIGN AND THEORETICAL ANALYSIS OF A PROTOTYPE TILTING-PAD RADIAL BEARING WITH ADJUSTABLE CLEARANCE

KONSTRUKCJA ORAZ ANALIZA TEORETYCZNA PROTOTYPOWEGO ŁOŻYSKA POPRZECZNEGO Z SEGMENTAMI WAHLIWYMI ORAZ REGULACJĄ LUZU

Key words: ORC turbo generator, tilting pad journal bearings, bearing clearance adjustment.

Abstract: The article introduces a design and analysis results of a prototype ORC (organic Rankine cycle) turbo generator rotor assembly of 300kW power, supported by tilting-pad bearings of original design. The calculations were performed for a prototype turbo generator rotor. The shaft of this machine is supported with two radial bearings, lubricated with an unusual lubricant – a low-boiling-point agent. The main objective of the presented research was to perform calculations verifying the feasibility of using hydrodynamic tilting-pad radial bearings with a low-viscosity lubricant to support a rather massive and high-speed rotor of the developed turbo generator and to determine the geometry and design of the bearings which would ensure optimal kinetostatic and dynamic properties of the rotating system, while simultaneously providing ease of assembly and smooth clearance adjustment.

Słowa kluczowe: turbogenerator ORC, łożyska ślizgowe wahliwe, regulacja luzu łożyska.

Streszczenie: W artykule przedstawiono konstrukcję oraz wyniki analiz teoretycznych zespołu wirnika prototypowego turbogeneratora ORC o mocy elektrycznej 300 kW podpartego w zaprojektowanych łożyskach z segmentami wahliwymi o oryginalnej konstrukcji. Obliczenia wykonano dla wirnika prototypowego turbogeneratora. Wał tej maszyny jest podparty w dwóch łożyskach poprzecznych, które są smarowane nietypowym czynnikiem smarnym – czynnikiem niskowrzącym. Podstawowym celem prezentowanych badań było obliczeniowe sprawdzenie możliwości zastosowania hydrodynamicznych poprzecznych łożysk z klockami wahliwymi i czynnikiem smarnym o małej lepkości do podparcia dość masywnego i wysokoobrotowego wirnika projektowanego turbogeneratora oraz wybór takiej geometrii i konstrukcji łożysk, która zapewniałaby najlepsze właściwości kinetostatyczne i dynamiczne układu wirującego przy jednoczesnym zachowaniu łatwości montażu i płynnej regulacji luzu.

INTRODUCTION

The aim of the research described in the article was to design an original bearing system of a prototype turbo generator with an electric power of 300kW in which the bearings are lubricated with a liquid low-boiling-point lubricant (supplied from the ORC system) designated MM. The developed turbo generator will be used to generate electricity from waste heat **[L. 1, 2]**. The use of a low-boiling-point agent as a lubricant in the discussed bearings enables the design of the ORC turbo generator in an "oil-free technology" **[L. 3]**, which means that the housing can be fully hermetic, and the only working medium inside will be a low-boiling-point agent (in the form of liquid or vapour). It should be emphasized that the use of a low-boiling-point agent to lubricate

[*] ORCID: 0000-0003-0819-0980. Gdańsk University of Technology, Faculty of Mechanical Engineering, G. Narutowicza 11/12 Street, 80-233 Gdańsk, Poland e-mail: artur.olszewski@pg.edu.pl.
[**] ORCID: 0000-0002-6848-5732. The Szewalski Institute of Fluid-Flow Machinery Polish Academy of Sciences, Turbine Dynamics and Diagnostics Department, Fiszera 14 Street, 80-231 Gdańsk, Poland, e-mail: gzywica@imp.gda.pl.
[***] ORCID: 0000-0003-2064-8739. Gdańsk University of Technology, Faculty of Mechanical Engineering, G. Narutowicza 11/12 Street, 80-233 Gdańsk, Poland, e-mail: tomasz.zochowski@pg.edu.pl.

hydrodynamic bearings is an unconventional solution **[L. 4]**. The MM low-boiling-point agent used in the ORC circuit has a very low viscosity, which causes problems when used as a lubricating fluid.

The difficulty of the undertaken task lies in developing a geometry and design of bearings which would be able to operate with low-viscosity liquid lubrication and meet the following design criteria:

- Stable operation of the rotor at a speed of 14,000 RPM;
- The ability to work properly with ORC liquid lubrication with a viscosity close to water; and,
- A minimum thickness of the lubricating film at nominal operating conditions at least 20 μm.

DESCRIPTION OF THE CALCULATIONS

Bearing and rotor model

The first stage of the work was to perform extensive computer simulations of the operation of bearings aimed at determining the optimal value of clearance, preload, pad length, as well as the number and position of the pads. This part of the article discusses the results of the analysis of the proposed bearings and the rotor which they support. The calculations were performed for the rotor of a prototype ORC turbo generator with an electric power of 300 kW. The shaft of this machine is supported with two radial bearings, which are lubricated with an unusual lubricant – a low-boiling-point agent. The main objective of the presented research was to perform calculations verifying the feasibility of using hydrodynamic tilting-pad radial bearings with a low-viscosity lubricant to support a rather massive and high-speed rotor of a 300 kW turbo generator, as well as to determine the geometry and design of the bearings which would ensure optimal kinetostatic and dynamic properties of the rotating system.

Bearing model

The calculations were performed for four geometry variants of the tilting-pad bearings. A common feature of all of the analysed bearings is the use of four evenly spaced tilting pads with symmetrical support (the pad is supported in the middle of its length). The angular span of each pad is 70°. The nominal diameter of all analysed bearings is 70 mm, and the width of the pads is 50 mm. It has also been assumed that the turbo generator bearings would be lubricated with a liquid low-boiling-point agent supplied from the ORC. The exact characteristics of all bearing variants are shown in **Figs. 1** and **2** and in **Table 1**. In Variants 2-1 and 2-2, all pads have been rotated by 45°, resulting in the distribution of the static load of the rotor on two lower pads. The variants with Annotation 1 are characterized by the lack of preload of the pads (preload = 0), while in the variants with Annotation 2, preload is present (preload = 0.5). This means that each pad is displaced by half the radial clearance towards the centre of the bearing.

During the analysis, it was assumed that the temperature of the low-boiling-point agent at the inlet of the bearings was 60°C. At this temperature, the MM low-boiling-point lubricant has the following density and dynamic viscosity: $\rho = 726.86$ kg/m^3, $\mu = 0.000335$ N·s/m^2. The use of a lubricant with such unfavourable properties requires a very thorough analysis and careful selection of appropriate bearing geometry.

As the presented calculations were preliminary, an isothermal model of a hydrodynamic bearing was used. This meant that the model did not take into account the increase in lubricant temperature in the bearing gap. It has been determined that, due to the negligible increase in temperature (resulting from the low viscosity of the lubricant), this model would be sufficiently accurate. The applied model takes into account the full geometry of the bearing, including the tilting of the pads. The parameters of the lubricant (low-boiling-point agent designated MM) at a temperature of 60°C and the static load on the bearings were also considered. The radial bearing on the side of the rotor plate (DE) was loaded with a force of 481 N and the bearing on the side of the thrust plate (NDE) was loaded with a force of 394 N.

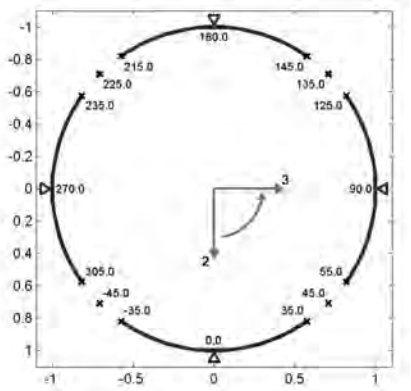

Fig. 1. Bearing diagram for Variants 1-1 and 1-2
Rys. 1. Schemat łożyska dla wariantów 1-1 i 1-2

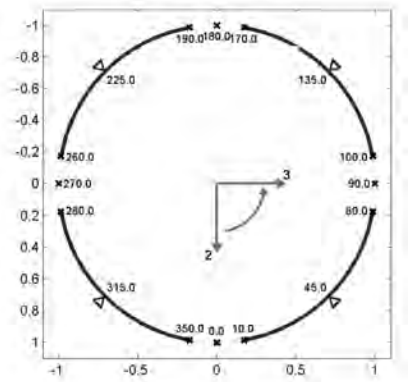

Fig. 2. Bearing diagram for Variants 2-1 and 2-2
Rys. 2. Schemat łożyska dla wariantów 2-1 i 2-2

Table 1. Characteristics of all variants of journal bearings
Tabela 1. Charakterystyka wszystkich wariantów łożysk poprzecznych

Technical parameters	Bearing variant			
	1-1	1-2	2-1	2-2
Shaft diameter [mm]	70	70	70	70
Bearing width [mm]	50	50	50	50
Number of pads	4	4	4	4
Pad support [%]	50	50	50	50
Angular span of one pad [°]	70	70	70	70
Preload (m)	0	50	0	50
Bearing clearance (Ψ)	0.0015	0.0025	0.0015	0.0025
Radial clearance (dR) [mm]	0.0525	0.0875	0.0525	0.0875
Radial clearance including preload (dR_{min}) [mm]	0.0525	0.04375	0.0525	0.04375

Rotor model

The calculations were performed in the specialized MADYN 2000 program, dedicated to the analysis of various types of bearings and rotors. This program is widely used to analyse rotor dynamics **[L. 9]** and has successfully passed experimental verification, both concerning small high-speed rotors **[L. 10]** and large turbine rotors **[L. 11]**. The FEM model of the rotor used for calculations is presented in **Fig. 3**. The model includes all the elements that may affect the kinetostatic and dynamic properties of the rotor-bearing system. Regarding parts of complex shape, such as a bladed rotor discs, the model assumes equivalent diameters taking into account the mass and moments of the inertia of the modelled elements.

At the free end of the shaft (left side in **Fig. 3**), there is a rotor plate of a single-stage axial micro turbine. The generator rotor sleeve is located in the central part of the shaft (between the bearings). On the other free end of the shaft (right side in **Fig. 3**), there is a retainer plate for a bidirectional thrust bearing. The total weight of the rotor is approximately 89 kg and its length is 1002 mm. The spacing between the bearings is 620 mm. The element with the largest diameter is the micro turbine rotor disc (its diameter is approx. 300 mm). The radial bearing journals have a diameter of 70 mm. The centre of gravity of the entire rotor is indicated with a green marker in **Fig. 3**. The nominal rotor speed is 14,000 RPM and the calculations were performed for a wide speed range of 2,000 to 30,000 RPM.

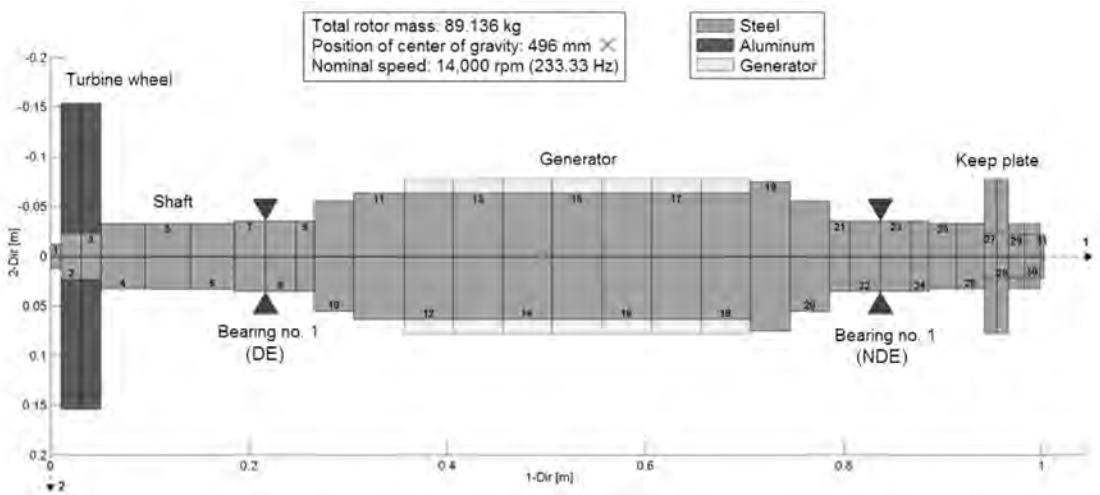

Fig. 3. FEM model of an ORC turbo generator rotor of 300 kW power
Rys. 3. Model MES wirnika turbogeneratora ORC o mocy 300 kW

CALCULATION RESULTS

This part of the article discusses selected calculation results. Due to the limited volume of this article, the following section presents detailed results for only one heavily loaded bearing located on the side of the rotor plate (DE). The results enable a direct comparison of the characteristics of different bearing design variants for the same load conditions. The presented results of rotor analysis were limited to only one variant in which radial bearings designated as 2-2 were used. These were the 50%-preload bearings with two pads supporting the bottom of the shaft.

Bearing characteristics

The characteristics of all variants of radial bearings were presented in a way that allows their direct comparison. **Figure 4** below shows the position of the journal centre depending on the rotational speed for different bearing variants. The lowest positions correspond to the lowest rotational speed, in this case, 2,000 RPM. As the rotational speed increases, the journal ascends. Successive positions of the journal were connected with each other with straight line segments. The highest analysed rotational speed was 30,000 RPM.

The results of the analysis indicate that bearing geometry has great influence on journal displacement and its position at various rotational speeds. In the case of the 1-1 variant, the position of the journal has been changing irregularly. Reaching analysis convergence has also been difficult for this variant, which demonstrates unfavourable conditions for the formation of a stable lubricating film. Some signs of unstable operation were also noted for Variant 2-1, but only in the top speed range. Moreover, in the range of lower speeds, the journal was moving along a straight line. A similar situation occurred in the case of Variants 1-2 and 2-2. For these bearings, the journal was moving along a vertical straight line through the centre of the bearing. It demonstrates stable operation of the system. For Variants 2-1 and 2-2, the initial position of the journal was further away from the centre of the bearing than for the corresponding Variants 1-1 and 1-2. This was due to a different support at the bottom of the journal. In Variants 1-1 and 1-2, the journal rested on one pad, and its support is located directly on the line along which the load was applied. In Variants 2-1 and 2-2, the journal was supported with two pads, the supports of which were at a distance from each other. Due to the tilting of the pads, the initial displacement of the journal from the centre of the bearing may have been greater than the nominal radial clearance, which is measured to the pad at its support. In the discussed example, this was the case at the lowest rotational speeds, when the thickness of the lubricating film was also the lowest (e.g., for Variant 2-1 the displacement of the journal centre at 2,000 rpm was about 60 μm with a nominal radial clearance of 52.5 μm).

Table 2 shows the calculated minimum thickness of the lubricating film depending on the rotational speed for different bearing variants. The thickness of the lubricating film varied in the range of 5 to 37 μm depending on the variant and the rotational speed. At the nominal speed (14,000 RPM), the highest thickness of the lubricating film occurred for Variant 1-1 (33 μm), and the lowest was for Variant 1-2 (24 μm). For Variant 2-1, it was 25 μm and, for Variant 2-2, it was 27 μm. At the lowest speeds, the thickness of the lubricating film was only a few micrometres. Such low thickness values of the lubricating film result from the low viscosity of the lubricant used.

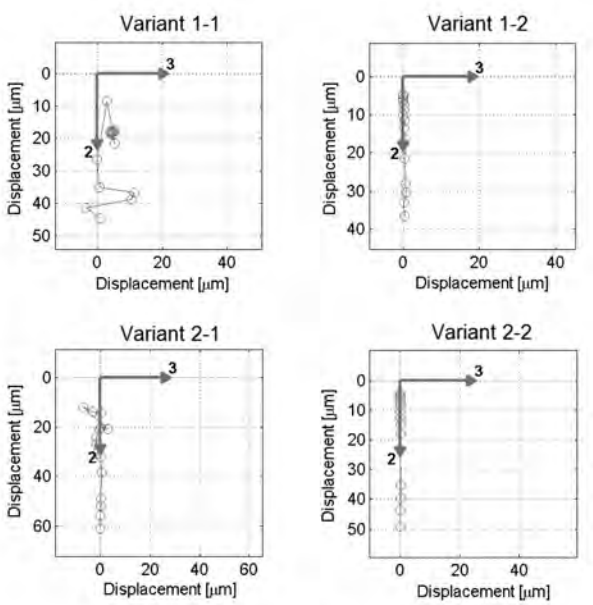

Fig. 4. Journal centre displacement depending on rotational speed for different bearing variants
Rys. 4. Zmiana położenia środka czopa w zależności od prędkości obrotowej dla różnych wariantów konstrukcyjnych łożyska

Table 2. Lowest bearing gap thickness in DE bearing depending on bearing variant
Tabela 2. Minimalna grubość szczeliny smarnej w łożysku DEw zależności od wariantu łożyska

Rotational speed		Bearing gap thickness [μm]			
[RPM]	[Hz]	Variant 1-1	Variant 1-2	Variant 2-1	Variant 2-2
2000	33.3	6	5	7	6
4000	66.7	9	8	10	10
6000	100	11	10	13	12
8000	133.3	13	12	15	14
10000	166.7	14	17	20	21
12000	200	21	21	25	25
14000	**233.3**	**33**	**24**	**25**	**27**
16000	266.7	26	26	27	28
18000	300	29	27	29	30
20000	333.3	29	29	32	31
22000	366.7	30	30	33	31
24000	400	30	30	30	32
26000	433.3	30	31	34	32
28000	466.7	30	32	36	33
30000	500	30	32	37	33

Figures 5–8 present the stiffness and damping characteristics of the analysed bearings. Separate graphs are shown for each bearing variant, with the main coefficients designated as 22 and 33 (respectively for the vertical and horizontal direction), while 23 and 32 denote the diagonal coefficients. Based on the obtained results, it can be concluded that changes in bearing geometry had a large impact on the dynamic characteristics. While the graphs of the damping coefficients seem to be similar (the main damping coefficients decrease with increasing speed), different values have been reached. This is especially noticeable at lower speeds. For example, at 2000 RPM for variant 2-2, the main damping coefficients equal $1.2 \cdot 10^5$ N·s/m, and, in the case of variant 1-1, the main damping coefficient d22 (vertical direction) equals $2.3 \cdot 10^5$ N·s/m. Even greater differences have been noted between the stiffness coefficients. Depending on the variant, not only were different values observed, but contrasting tendencies as well (values increased or decreased with increasing speed). In the cases of Variants 2-1 and 2-2, the stiffness and damping coefficients determined for the perpendicular directions are equal, which results from the symmetry of the shaft support. For all the analysed bearings, the diagonal coefficients reached values close to zero, which is typical for tilting-pad bearings. The only deviations from this rule were noticed at higher speeds in the case of Variant 2-1.

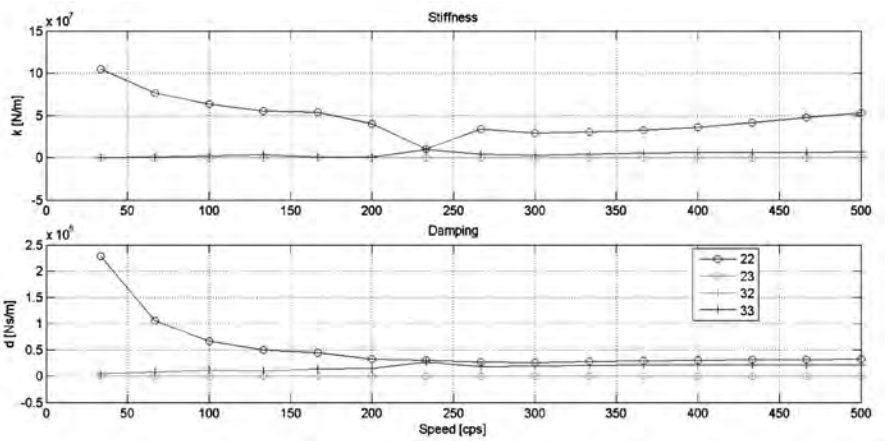

Fig. 5. Stiffness and damping coefficients for bearing Variant 1-1
Rys. 5. Przebiegi współczynników sztywności i tłumienia dla łożyska wg wariantu 1-1

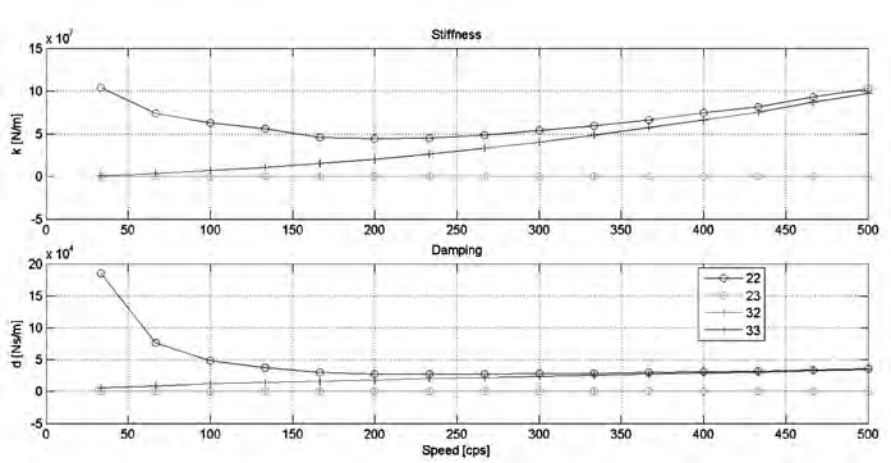

Fig. 6. Stiffness and damping coefficients for bearing Variant 1-2
Rys. 6. Przebiegi współczynników sztywności i tłumienia dla łożyska wg wariantu 1-2

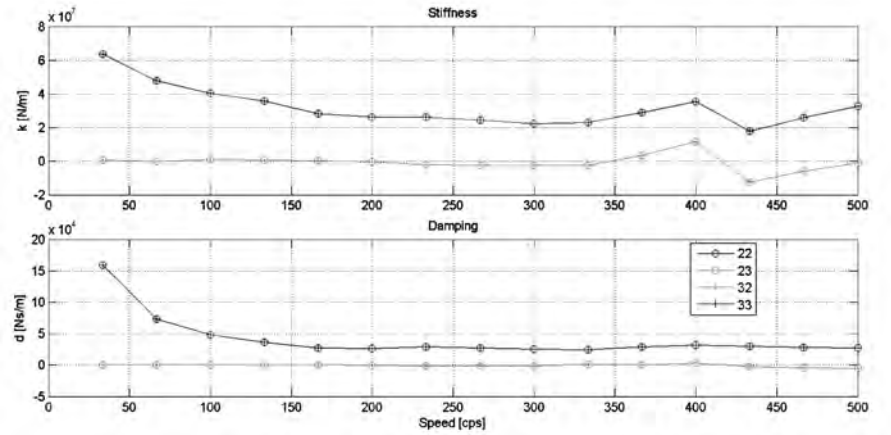

Fig. 7. Stiffness and damping coefficients for bearing Variant 2-1
Rys. 7. Przebiegi współczynników sztywności i tłumienia dla łożyska wg wariantu 2-1

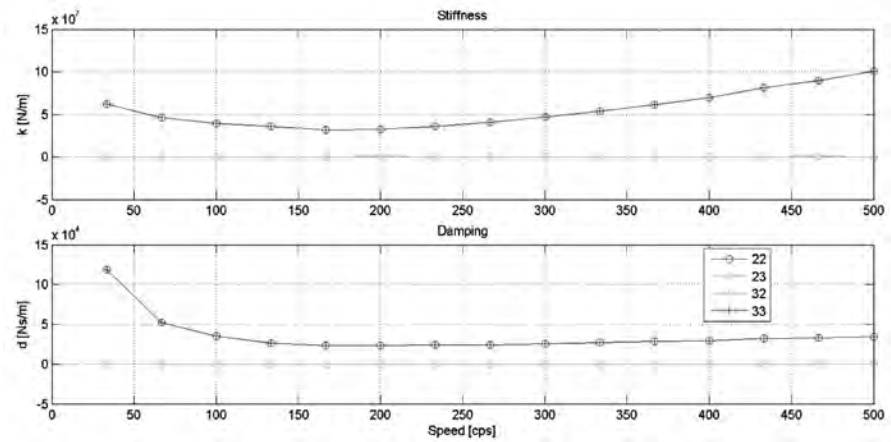

Fig. 8. Stiffness and damping coefficients for bearing Variant 2-2
Rys. 8. Przebiegi współczynników sztywności i tłumienia dla łożyska wg wariantu 2-2

Rotor analysis results

The rotor analysis included both kinetostatic and dynamic calculations. They were performed for all bearing design variants. Regardless of the bearing variant, the kinetostatic load did not change, because both the rotor mass distribution and the bearing position were the same. The load on the bearing closer to the impeller was 481 N, and, on the bearing at the free end of the shaft, it was approx. 393 N. The results of the kinetostatic analysis have also demonstrated that both the bending moments and the shear forces in the shaft were very low. Furthermore, the reduced stresses in the shaft cross-sections could be considered negligible, since they did not exceed the value of 1 MPa. Certain differences between the calculation results for different bearing variants could be noticed in terms of kinetostatic displacements. At the nominal speed, the displacement of the end of the shaft on which the micro turbine rotor disc is located reached a maximum of 34 μm (Variant 2-1). The smallest displacement at this point at nominal speed was obtained for Variant 1-2, and it was 16 μm. Differences in the displacements of the shaft loaded in the same way are the result of different stiffness values of the bearings.

As part of the rotor dynamic analysis, calculations including modal analysis and forced vibration analysis were performed. The stiffness and damping factors for radial bearings, discussed in the previous section were taken into account. The modal analysis was performed in the frequency range up to 500 Hz, which was chosen in such a way as to include frequencies twice as high as the nominal rotational frequency of the rotor. Due to the limited volume of this article, the presented calculation results involve only the rotor supported on bearing Variant 2-2. These bearings have performed stably over the entire RPM range. Because the results obtained for the other bearing variants were similar (which is a consequence of similar values of dynamic coefficients), the presented results can be treated as representative for the entire group of analysed bearings.

Seven modes of free vibrations of the rotor-bearing system were revealed in the analysed frequency range, with four modes occurring at lower frequencies being strongly damped (damping above 50%). The remaining three modes are characterized by much weaker damping. At the lowest frequency, there was a vibration mode related to the rotation of the entire undistorted rotor about its own axis (at a frequency of 9.3 Hz). Its frequency results from the mass of the shaft and the stiffness of the support in the direction of the rotation. Stiffness in this direction has been assumed arbitrarily; therefore, this mode of vibration has no practical significance in this case. The remaining modes of vibrations are presented graphically in the figures below (**Figs. 9–14**).

The vibration modes shown in **Figs. 9–12** correspond to the transverse vibrations of the rotor in the bearings as a rigid body or with slight bending (these are

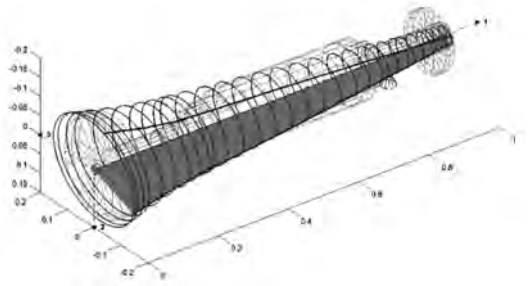

Fig. 9. Transverse rotor vibration at 133.2 Hz (damping 27.3%)

Rys. 9. Drgania poprzeczne wirnika przy częstotliwości 133,2 Hz (tłumienie 27,3%)

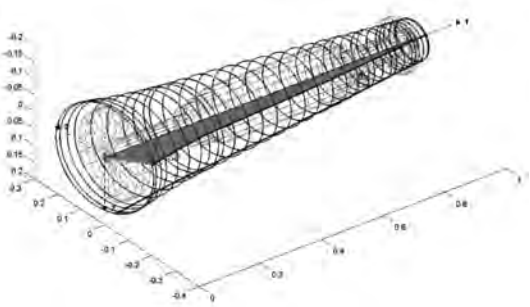

Fig. 10. Transverse rotor vibration at 134.2 Hz (damping 28.2%)

Rys. 10. Drgania poprzeczne wirnika przy częstotliwości 134,2 Hz (tłumienie 28,2%)

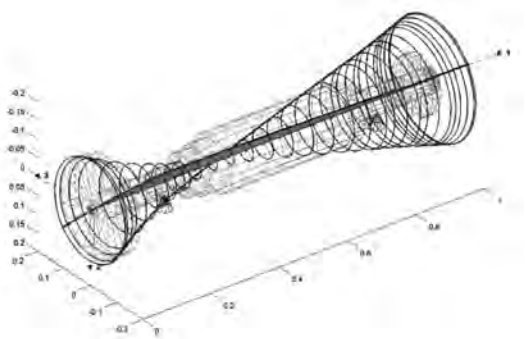

Fig. 11. Transverse rotor vibration at 157.6 Hz (damping 32.5%)

Rys. 11. Drgania poprzeczne wirnika przy częstotliwości 157,6 Hz (tłumienie 32,5%)

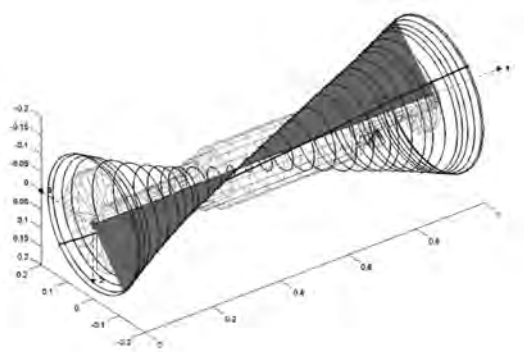

Fig. 12. Transverse rotor vibration at 171.2 Hz (damping 34.6%)

Rys. 12. Drgania poprzeczne wirnika przy częstotliwości 171,2 Hz (tłumienie 34,6%)

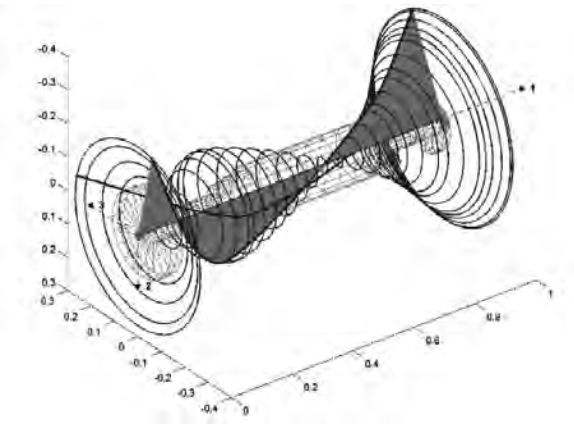

Fig. 13. Transverse rotor vibration at 358.8 Hz (damping 10.8%)

Rys. 13. Drgania poprzeczne wirnika przy częstotliwości 358,8 Hz (tłumienie 10,8%)

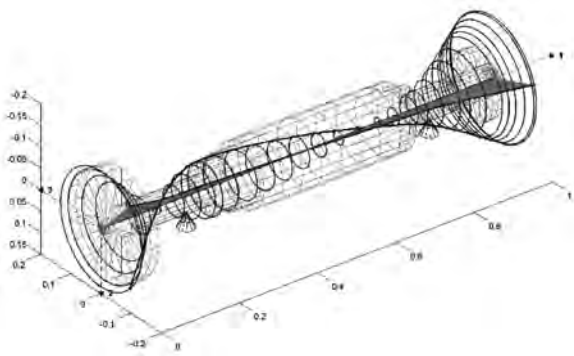

Fig. 14. Transverse rotor vibration at 455.5 Hz (damping 6.7%)

Rys. 14. Drgania poprzeczne wirnika przy częstotliwości 455,5 Hz (tłumienie 6,7%)

the "cylindrical and conical" forms of vibration). Figures 13 and 14 show the modes of bending vibrations. They occur at frequencies of 358.8 Hz and 455.5 Hz. As the nominal rotational frequency is 233.3 Hz, the analysed rotor can be considered subcritical. This is advantageous in terms of the dynamics of the system and should help maintain low level of vibrations in the entire operating speed range. In the analysed frequency range, there was no form of torsional vibrations of the rotor. Similar results of modal analysis were also obtained for the remaining three bearing variants.

As part of the calculations, forced vibration analysis of the rotor was also performed, enabling the investigation of vibration levels in various areas of the rotor in a wide range of rotational speeds and allowing the assessment of the influence of individual vibration modes on the dynamic characteristics of the system. The calculations were performed with the assumption that the maximum allowable system imbalance (assumed according to ISO1940-1) would be represented by one additional concentrated mass located in the middle of the rotor, near the centre of gravity (see **Fig. 3**).

The obtained amplitude-phase characteristic (**Fig. 15**) demonstrates the low level of rotor vibrations below the nominal speed (vibration amplitude does not exceed 5 μm). The highest vibration level occurs at the end of the shaft on which the micro turbine disc is located. In the range from 8,000 RPM to 10,000 RPM, the gradually increasing vibrations plateaued at a certain level. In this speed range, significant changes in the vibration phase were also observed. This was related to the previously discussed modes of transverse vibrations of the rotor; however, because of strong damping effect,

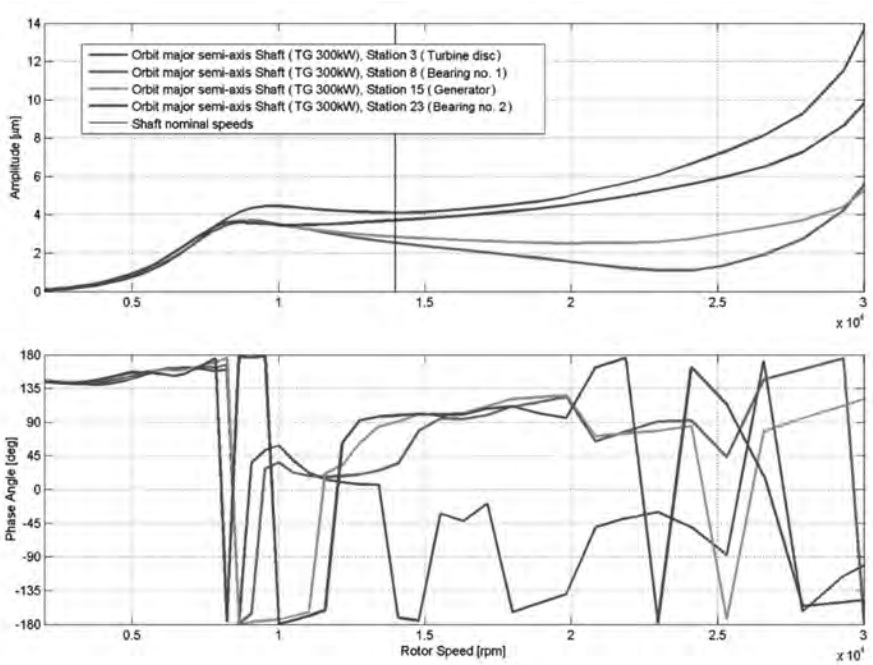

Fig. 15. Amplitude-phase characteristic of rotor supported with Variant 2-2 bearings

Rys. 15. Charakterystyka amplitudowo-fazowa wirnika podpartego w łożyskach wg wariantu 2-2

it did not cause a significant increase in the overall vibration level. The increase of the rotational speed up to the nominal speed did not cause a significant vibration level raise, until further increase, where it became most noticeable from approx. 20,000 RPM (i.e. well above the nominal speed). At the highest analysed speed (30,000 RPM), the maximum amplitude of rotor vibrations did not exceed 14 μm, and, as before, it occurred on the micro turbine rotor disc. In general, based on the conducted analysis, it can be concluded that the rotor is characterized by stable operation and low vibrations remaining at an entirely acceptable level.

As in the case of the modal analysis, the results of the forced vibration analysis were quite similar for different bearing variants. Therefore, they have not been presented and discussed in detail. Essentially, it can be stated that the proposed tilting-pad bearings lubricated with a liquid low-boiling-point agent provide very good dynamic properties of the rotating system in the entire operating speed range. In this speed range, the rotor remains subcritical and the vibration level is very low.

PROTOTYPE RADIAL BEARING DESIGN

After the process of optimizing the bearing geometry has been completed, its design and production technology were developed according to Variant 2-1. Based on the literature data and previously conducted research **[L. 5–8]**, PEEK has been chosen as the sliding layer material, demonstrating excellent tribological properties when lubricated with low-viscosity liquids.

The most substantial design problem was to achieve the actual radial clearance of about 0.05 mm. The total bearing clearance is influenced by the actual dimension of the inner diameter of the bearing housing, the outer diameter of the pads in contact with the body, and the diameter of the sliding layer. The sum of these three dimensions affects the actual bearing clearance and thus the characteristics of the hydrodynamic film. Achieving such a small value of the actual clearance within the tolerance of about ±0.01mm is technically unattainable for classic tilting-pad bearings. This is not the case with classic oil-lubricated bearings, as the tolerance requirements of individual bearing elements may be relatively relaxed due to the significant thickness of the oil film.

The finished bearing is shown in **Fig. 16**. It consists of 4 tilting pads (1), each pad supported on an adjustment mechanism (2). The pads are encased inside a housing (3), to which cover plates (4) are attached. Holes in the plates allow the pads to tilt and enable limited movement in the radial direction (necessary for their adjustment). The precision of the adjustment mechanism allows achieving the desired position of the segments with an accuracy of a few micrometres, and the principle of its operation is based on the use of a differential screw (full rotation causes a displacement of 250 micrometres). The adjustment is performed with a bronze screw (5), which is screwed into a pusher prevented from rotating (not visible in the photo), whose front surface contacts and supports the pad. For initial positioning of the pads in relation to the housing axis, a precise control journal and a centring tool are used, which position the journal in the axis of the bearing housing.

The lubricant is supplied to a circumferential groove (6) in the housing, from which it flows through axial grooves (7) to spray holes (8) distributed between the segments. The bearing housing is sealed with two O-rings (9) and attached to the machine body with four peripheral bolts.

Fig. 16. Photo of the complete bearing
Rys. 16. Zdjęcie kompletnego łożyska

SUMMARY

The article discusses the results of an analysis concerning a 300 kW prototype ORC turbo generator supported with newly designed bearings lubricated with a low-boiling-point lubricant. The bearings utilize tilting pads made of carefully selected synthetic material, which should enable their proper operation despite the low thickness of the lubricating film. The conducted analysis allows for the following conclusions:

1. Hydrodynamic tilting-pad radial bearings lubricated with the MM low-boiling-point agent performed well, although Variants 1-1 and 2-1 displayed some difficulties related to the formation of stable lubricating film at certain RPM. All bearing variants operated with very thin bearing gaps, which was especially noticeable at lower RPM.
2. Regardless of the bearing variant, the turbo generator rotor was characterized by satisfactory dynamic properties. This was a result of its high stiffness, leading to the first critical speed related to bending vibration being far outside of the operating speed range.

3. Based on the performed analysis, the authors recommend two bearing variants for further production – 1-2 and 2-2. These are the bearings where initial preload was applied, which was beneficial for their characteristics.
4. The performed work has resulted in the design and prototype construction of bearings with smoothly adjustable clearance. Considering the ingenuity of the involved solutions, the developed design has been applied for patenting at the Polish Patent Office.

The presented research has been conducted as a part of the POIR.01.01.01-00-0414/17 project titled: "Development of the first Polish prototype medium-power 300kW ORC generator using industrial waste heat" executed by MARANI Sp. z o.o.

REFERENCES

1. Kiciński J., Żywica G.: Steam microturbines in distributed cogeneration, Springer International Publishing, 2014.
2. Witanowski Ł., Klonowicz P., Lampart P., Suchocki T., Jędrzejewski Ł., Zaniewski D., Klimaszewski P.: Optimization of an axial turbine for a small scale ORC waste heat recovery system, ENERGY 2020, 205, 118059.
3. Kozanecki Z., Kozanecka D., Łagodziński J., Tkacz E.: Numerical and Experimental Investigations of Oil-Free Support Systems to Predict High-Speed Rotor Bearing Dynamics, Journal of Vibration Engineering & Technologies 2015, 3(6), pp. 759–768.
4. Żywica G., Bagiński P.: Investigation of unconventional bearing systems for microturbines, Advances in Mechanism and Machine Science, IFToMM WC 2019, Mechanisms and Machine Science 2019, 73, pp. 3439–3448.
5. Wodtke M.: Hydrodynamiczne łożyska wzdłużne z warstwą ślizgową PEEK, Monografia, Gdańsk 2017.
6. Olszewski A.: Studia nad czynnikami wpływającymi na obciążalnośći charakterystyki tribolgiczne poprzecznych hydrodynamicznych łożysk ślizgowych smarowanych wodą, Monografia, Gdańsk 2017.
7. San Andrés L.: Analysis of tilting pad bearings., Class Notes 16 – Modern Lubrication, Texas 2010.
8. Gliwiński J., Łuczywo J., Olszewski A., Wasilczuk M., Żochowski T.: Preliminary testing of peekpocket journal bearing, raport z badań, niepublikowany.
9. Schmied J., Perucchi M., Pradetto J.C.: Application of MADYN 2000 to rotordynamic problems of industrial machinery, ASME Turbo Expo 2007, Montreal (Canada), GT2007-27302.
10. Fuchs A., Klimpel T., Schmied J., Rohne K.H.: Comparison of measured and calculated vibrations of a turbocharger, SIRM 2017 Conference, Graz (Austria).
11. Matthys K., Perucchi M., De Bauw K.: Rotor dynamic modelling as a powerful support tool for vibration analysis on large turbomachinery, IFToMM International Conference on Rotor Dynamics 2010, Seoul (Korea).